DOPING VARIATION AT THE TCO/A-SI(P) HOLE CONTACT

Christoph Luderer[a], Leonard Tutsch[a], Christoph Messmer[a,b], Martin Hermle[a], Martin Bivour[a]

[a] Fraunhofer Institute for Solar Energy Systems (ISE), Heidenhofstrasse 2, 79110 Freiburg, Germany
[b] Department of Sustainable Systems Engineering (INATECH), Albert Ludwig University of Freiburg, Georges-Köhler-Allee 103, D-79110 Freiburg, Germany

ABSTRACT: Resistive losses arise at the transport barriers at the interfaces between the different semiconductor materials in the TCO/a-Si/c-Si stack and limit the power output of silicon heterojunction (SHJ) solar cells. A key element is the unisotype recombination junction at the TCO/a-Si(p) interface. We identify sufficient doping on both sides of this junction to be crucial for low contact resistance (ρ_c). For a-Si this is achieved by using a sufficient but not too high doping gas concentration during deposition. On the TCO side high oxygen (O_2) gas concentration during deposition have to be avoided. To combine high transparency of O_2-rich TCOs with low ρ_c and R_{sheet} of O_2-poor TCOs, we utilize a TCO layer stack. We show that a low O_2 content in the vicinity of the TCO/a-Si(p) interface is mandatory to provide efficient tunnelling transport and to avoid resistive losses at the TCO/a-Si(p) interface.
Keywords: Silicon Heterojunction, Amorphous silicon, Doping, Contact resistivity

1 INTRODUCTION

Silicon heterojunction (SHJ) solar cells hold the current world record efficiency for silicon single junction solar cells [1]. One of the remaining limitations are the significant resistive losses originating at the critical TCO/a-Si and a-Si/c-Si junctions [2, 3]. The contact resistivity (ρ_c) at the hole contact is one of the main contributors to the cell's series resistance (R_s) [4, 5]. The unisotype recombination junction at the TCO/a-Si(p) interface relies on efficient tunnelling transport, either via direct tunnelling or facilitated via trap states within the band gap (trap-assisted tunnelling, TAT) [6–8].

Optimizing transport in SHJ is governed by the trade-off between optical and electrical properties. On the TCO side, transparency and conductivity can be tuned via the TCO oxygen (O_2) content [9]. While high-mobility TCOs with μ_{TCO} > 100 cm²/Vs allow the reduction of charge carrier concentration (N_{TCO}) for higher transparency while maintaining high lateral conductivity [10], issues regarding rather high ρ_c have been reported [11]. One approach to decouple optical and electrical as well as bulk and interface properties, is to utilize layer stacks [11–13].

In this contribution we present a thorough investigation of the ITO/a-Si(p) contact resistivity. First, the optimum a-Si doping regarding ρ_c is determined. Second, ρ_c is screened over a wide range of ITO O_2 contents. We show that, aside lateral transport (R_{sheet}), vertical transport (ρ_c) can also be strongly effected for highly transparent but low conductive TCOs. Finally, the beneficial effect on ρ_c of an O_2-poor ITO interlayer combined with an O_2-rich "bulk" ITO is presented. For our more detailed investigation of the influence of doping on SHJ contacts including numerical device simulations and solar cell results we refer to [14].

2 EXPERIMENTAL

Fig. 1 shows sketches of the resistance test structures that were utilized to evaluate the TCO/a-Si contact resistance. The basic fabrication is described in [3]. To realize the doping variation within a-Si(p), the trimethylborane (TMB) gas concentration during plasma-enhanced chemical vapor deposition (PECVD) was varied while the total gas flow and all other deposition parameters were fixed. The ITO doping was changed via the O_2 content in the sputtering gas during deposition. In both cases, the deposition time was adapted to reach a comparable layer thickness for all groups. TCO layer properties for films on glass substrates were obtained from Hall effect measurements using the van der Pauw's method. Prior to the *I-V* measurements, the structures were annealed on a Präzitherm hotplate in ambient air at 180 °C for 10 min. Two-terminal *I-V* measurements were performed on a WAVELABS Sinus-220 at 25 °C.

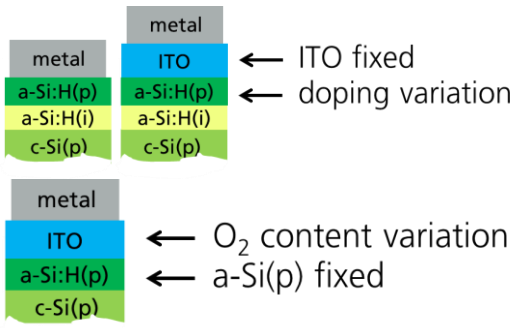

Figure 1: Sketch of the used resistance test structures. The intrinsic a-Si layer was omitted for the ITO O_2 content variation to be more sensitive to the TCO/a-Si contact. The rear contact of all groups comprised only boron doped a-Si with fixed doping concentration and full area metallization.

3 RESULTS

The dependence of ρ_c on the TMB gas concentrations is shown in Fig 2. An optimum was observed at a doping gas concentration of 3 % for samples with ITO (dotted lines) and without ITO (solid lines). Optimum ρ_c was 150 mΩ·cm² without and 200 mΩ·cm² with ITO. The increase in ρ_c due to ITO was lowest at 3 % (+50 mΩ·cm²) and significantly higher at lowest

(+200 mΩ·cm²) or highest TMB gas concentration (+500 mΩ·cm²). The optimum doping concentrations of TMB was used for the ITO O_2 content variation and the ITO stacks in the following sections.

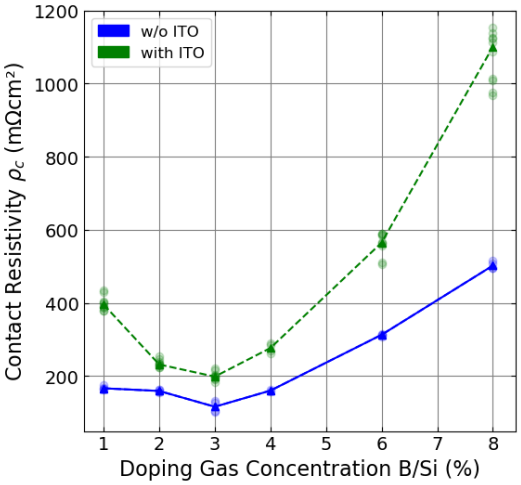

Figure 2: Contact resistivity ρ_c of hole contact stacks with and without ITO after 180 °C annealing as a function of TMB gas concentration. Dotted and solid lines are meant as guide to the eye.

The influence of the O_2 content on ρ_c is depicted in Fig. 3. ρ_c was rather constant in the range of 0-1.6 % O_2 content. Lowest ρ_c values were obtained for ITO deposited with a medium O_2 content of 1.6 %, but no clear optimum could be resolved due to wafer to wafer scattering. For highly transparent ITO with high O_2 content ρ_c increased significantly. ITO sheet resistances displayed at the top x-axis were measured on glass in the as deposited state. Similarly to ρ_c, R_{sheet} increased with rising ITO O_2 content.

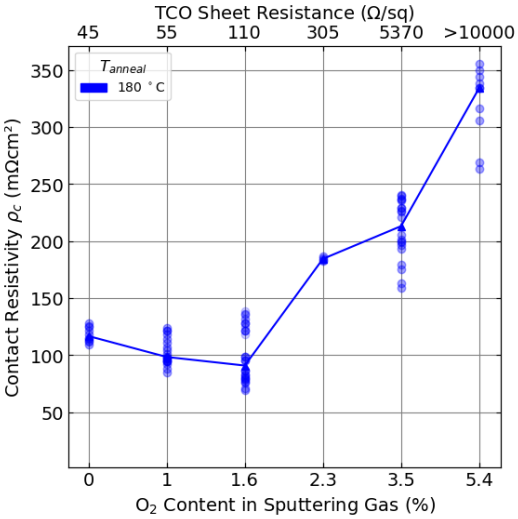

Figure 3: Contact resistivity ρ_c of hole contact stacks after 180 °C annealing including ITO with varying O_2 content. The solid line is meant as guide to the eye.

Fig. 4 shows again the increased ρ_c of O_2-rich ITO (3.5 %, group 2) compared to medium-O_2 ITO (1.6 %, group 1). By inserting a 20 nm-thick O_2-poor ITO (1.0 % O_2) interlayer between a-Si(p) and the O_2-rich ITO, the ρ_c was reduced by about 60 mΩ·cm² (group 3) to nearly the same value as for the single layer medium-O_2 ITO (1.6 %, group 1). When the 20 nm-thick O_2-poor ITO (1.0 % O_2) interlayer was inserted at the metal/ITO interface, the ρ_c was also reduced to a value of 100 mΩ·cm^2 (group 4)).

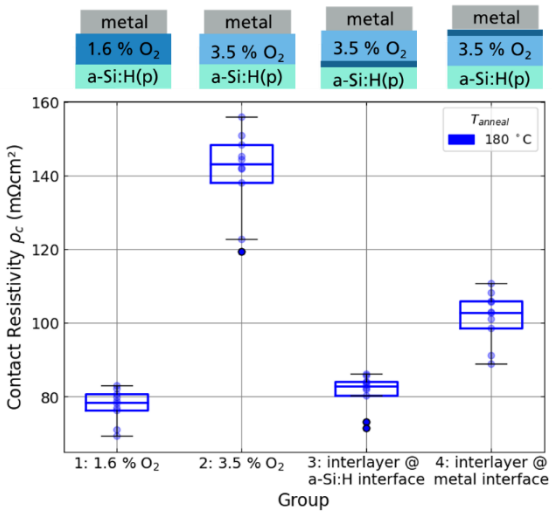

Figure 4: Contact resistivity ρ_c of different and hole contact heterojunction stacks, as depicted above, after 180 °C annealing.

4 DISCUSSION

In case of the a-Si doping variation in Fig. 2, ρ_c is expected to be lowest for a-Si with the highest active dopant concentration. For too low TMB concentration not enough dopants are incorporated in the a-Si layer. For too high TMB concentrations the increased defect density drastically lowers the doping efficiency [15–17]. In both cases, the active dopant concentration is insufficient to provide proper hole conductivity via induced c-Si band bending in the contact region [8, 18]. Additionally, the TCO/a-Si(p) contact suffers from insufficient a-Si doping. This contact relies heavily on tunnelling transport. As the charge carrier concentration $N_{a\text{-}Si(p)}$ decreases with non-optimal doping, the depletion width and therefore the barrier width increases. This reduces the tunnel probability, hence ρ_c of the TCO/a-Si(p) contact increases.

On the TCO side, in principle, exists a trade-off for hole contact transport between high N_{TCO} at low O_2 content and better work function matching to a-Si(p) at high O_2 content. In [13, 19] it was shown, that the ITO work function could indeed be tailored by varying the O_2 content to either facilitate hole or electron extraction. However, on device level, transport was not improved with higher O_2 content. Similarly, in Fig. 3 ρ_c increased with rising O_2 content. Thus, is seems that the less efficient tunnelling at high O_2 content is more relevant for the contact resistance, as the better work function matching at the TCO/a-Si(p). In addition to reduced tunnel probability due to reduced N_{TCO}, the formation of a resistive interlayer might also impede transport [19]. Considering the negative Gibbs formation energy for the silicon oxidation reaction at the ITO/a-Si interface [20, 21], the formation of a silicon oxide layer upon TCO

growth is feasible [13, 19, 22, 23]. During the annealing step this silicon oxide might thicken or densify further.

To combine high transparency and low resistance for solar cell application, an ITO stack was utilized (Fig. 4). During the annealing step the O_2 content in the ITO stack might balance and result in an ITO with overall lower O_2 content compared to the reference without interlayer, explaining the lower overall ρ_c with such an interlayer. However, the comparison between groups 3 and 4 in Fig. 4 shows that in particular at the ITO/a-Si interface the O_2 content has to be low respectively N_{TCO} has to be high for low ρ_c. Moreover, similar results were obtained with twice the O_2-rich ITO thickness and even thinner O_2-poor ITO interlayers down to 4 nm [14]. Thus, ρ_c is rather governed by properties in the vicinity of the TCO/a-Si interface than ITO "bulk" properties. The reason for the improved ITO/a-Si(p) contact with such an O_2 poor interlayer could be (i) enhanced tunnel probability due to higher N_{TCO} at the interface, (ii) the avoidance or the less pronounced formation of an resistive layer at the interface due to the lower oxygen content or (iii) a combination of (i) and (ii).

5 CONCLUSION

The hole contact resistivity of SHJ stacks was studied with respect to doping on both sides of the ITO/a-Si(p) junction. On the a-Si(p) side, an optimum regarding ρ_c was found when sufficient but not too high doping gas concentration during deposition was used. On the ITO side, increasing O_2 content lead to increased ρ_c due to reduced N_{TCO} and/or the formation of a resistive interlayer. It could be shown that the use of a thin layer of low-O_2 ITO at the ITO/a-Si(p) interface decreases ρ_c and relaxes the trade-off between optical and electrical TCO properties. The use of such a TCO stack can lead to improved power conversion efficiency on cell level.

6 ACKNOWLEDGMENT

The authors would like to thank A. Leimenstoll, F. Schätzle, K. Zimmermann for sample preparation and D. Kurt and Z. Newcomb-Hall for sample preparation and dark *I-V* measurements.

This work was funded by the German Federal Ministry for Economic Affairs and Energy under contract N° 03EE1032 (CUSTCO) within the SOLAR-ERA.NET program.

References

[1] K. Yoshikawa, W. Yoshida, T. Irie, H. Kawasaki, K. Konishi, H. Ishibashi, T. Asatani, D. Adachi, M. Kanematsu, H. Uzu, and K. Yamamoto, "Exceeding conversion efficiency of 26% by heterojunction interdigitated back contact solar cell with thin film Si technology," *Solar Energy Materials and Solar Cells*, vol. 173, pp. 37–42, 2017.

[2] T. F. Schulze, L. Korte, E. Conrad, M. Schmidt, and B. Rech, "Electrical transport mechanisms in a-Si: H/c-Si heterojunction solar cells," *Journal of Applied Physics*, vol. 107, no. 2, p. 23711, https://aip.scitation.org/doi/pdf/10.1063/1.3267316?class=pdf, 2010.

[3] C. Luderer, C. Messmer, M. Hermle, and M. Bivour, "Transport Losses at the TCO/a-Si:H/c-Si Heterojunction: Influence of Different Layers and Annealing," *IEEE J. Photovoltaics*, vol. 10, no. 4, pp. 1–7, 2020.

[4] D. Lachenal, D. Baetzner, W. Frammelsberger, B. Legradic, J. Meixenberger, P. Papet, B. Strahm, and G. Wahli, "Heterojunction and Passivated Contacts: A Simple Method to Extract Both n/tco and p/tco Contacts Resistivity," *Energy Procedia*, vol. 92, pp. 932–938, 2016.

[5] L. Basset, W. Favre, D. Munoz, and J. P. Vilcot, "Series Resistance Breakdown of Silicon Heterojunction Solar Cells Produced on CEA-INES Pilot Line," in *Proc. 35th Eur. Photovolt. Sol. Energy Conf. Exhib.*, Brussels, 2018.

[6] P. Procel, H. Xu, A. Saez, C. Ruiz-Tobon, L. Mazzarella, Y. Zhao, C. Han, G. Yang, M. Zeman, and O. Isabella, "The role of heterointerfaces and subgap energy states on transport mechanisms in silicon heterojunction solar cells," *Prog Photovolt Res Appl*, 2020.

[7] S. Kirner, M. Hartig, L. Mazzarella, L. Korte, T. Frijnts, H. Scherg-Kurmes, S. Ring, B. Stannowski, B. Rech, and R. Schlatmann, "The Influence of ITO Dopant Density on J-V Characteristics of Silicon Heterojunction Solar Cells: Experiments and Simulations," *Energy Procedia*, vol. 77, pp. 725–732, https://depositonce.tu-berlin.de/bitstream/11303/7616/1/1-s2.0-S1876610215008711-main.pdf, 2015.

[8] C. Messmer, M. Bivour, J. Schön, and M. Hermle, "Requirements for efficient hole extraction in transition metal oxide-based silicon heterojunction solar cells," *Journal of Applied Physics*, vol. 124, no. 8, p. 85702, 2018.

[9] B. G. Lewis and D. C. Paine, "Applications and Processing of Transparent Conducting Oxides," *MRSBulletin*, vol. 25, no. 8, 2000.

[10] T. Koida, H. Fujiwara, and M. Kondo, "Hydrogen-doped In2O3 as High-mobility Transparent Conductive Oxide," *Jpn. J. Appl. Phys.*, vol. 46, no. No. 28, L685-L687, 2007.

[11] L. Barraud, Z. C. Holman, N. Badel, P. Reiss, A. Descoeudres, C. Battaglia, S. de Wolf, and C. Ballif, "Hydrogen-doped indium oxide/indium tin oxide bilayers for high-efficiency silicon heterojunction solar cells," *Solar Energy Materials and Solar Cells*, vol. 115, pp. 151–156, 2013.

[12] M. Leilaeioun, W. Weigand, M. Boccard, Z. J. Yu, K. Fisher, and Z. C. Holman, "Contact Resistivity of the p-Type Amorphous Silicon Hole Contact in Silicon Heterojunction Solar Cells," *IEEE J. Photovoltaics*, pp. 1–9, 2019.

[13] M. Bivour, *Silicon heterojunction solar cells: Analysis and basic understanding*. Stuttgart: Fraunhofer Verlag, 2015.

[14] C. Luderer, L. Tutsch, C. Messmer, M. Hermle, and M. Bivour, "Influence of Thin Film Doping on SHJ Contact Resistivity," *IEEE J. Photovoltaics*, submitted.

[15] M. Stutzmann, D. K. Biegelsen, and R. A. Street, "Detailed investigation of doping in hydrogenated

amorphous silicon and germanium," *Phys. Rev. B*, vol. 35, no. 11, pp. 5666–5701, 1987.

[16] R. A. Street, "Localized states in doped amorphous silicon," *Journal of Non-Crystalline Solids*, vol. 77-78, pp. 1–16, 1985.

[17] L. Korte, E. Conrad, H. Angermann, R. Stangl, and M. Schmidt, "Advances in a-Si:H/c-Si heterojunction solar cell fabrication and characterization," *Solar Energy Materials and Solar Cells*, vol. 93, no. 6-7, pp. 905–910, 2009.

[18] U. Würfel, A. Cuevas, and P. Würfel, "Charge Carrier Separation in Solar Cells," *IEEE J. Photovoltaics*, vol. 5, no. 1, pp. 461–469, http://ieeexplore.ieee.org/ielx7/5503869/6991619/06960066.pdf?tp=&arnumber=6960066&isnumber=6991619, 2015.

[19] C. Messmer, M. Bivour, C. Luderer, L. Tutsch, J. Schon, and M. Hermle, "Influence of Interfacial Oxides at TCO/Doped Si Thin Film Contacts on the Charge Carrier Transport of Passivating Contacts," *IEEE J. Photovoltaics*, vol. 10, no. 2, pp. 343–350, 2020.

[20] L. G. Gerling, C. Voz, R. Alcubilla, and J. Puigdollers, "Origin of passivation in hole-selective transition metal oxides for crystalline silicon heterojunction solar cells," *J. Mater. Res.*, vol. 32, no. 02, pp. 260–268, 2017.

[21] M. T. Greiner, L. Chai, M. G. Helander, W.-M. Tang, and Z.-H. Lu, "Metal/Metal-Oxide Interfaces: How Metal Contacts Affect the Work Function and Band Structure of MoO 3," *Adv. Funct. Mater.*, vol. 23, no. 2, pp. 215–226, 2013.

[22] M. Wimmer, M. Bär, D. Gerlach, R. G. Wilks, S. Scherf, C. Lupulescu, F. Ruske, R. Félix, J. Hüpkes, G. Gavrila, M. Gorgoi, K. Lips, W. Eberhardt, and B. Rech, "Hard x-ray photoelectron spectroscopy study of the buried Si/ZnO thin-film solar cell interface: Direct evidence for the formation of Si–O at the expense of Zn-O bonds," *Appl. Phys. Lett.*, vol. 99, no. 15, p. 152104, 2011.

[23] L. Tutsch, F. Feldmann, J. Polzin, C. Luderer, M. Bivour, A. Moldovan, J. Rentsch, and M. Hermle, "Implementing transparent conducting oxides by DC sputtering on ultrathin SiOx / poly-Si passivating contacts," *Solar Energy Materials and Solar Cells*, vol. 200, p. 109960, 2019.